Organic & Biomolecular Chemistry

Dynamic Article Links

Cite this: *Org. Biomol. Chem.*, 2011, **9**, 6133

www.rsc.org/obc

PAPER

Synthesis, biological evaluation and structural characterization of novel glycopeptide analogues of nociceptin N/OFQ†‡

Gemma Arsequell,[a] Mònica Rosa,[a] Carlos Mayato,[b] Rosa L. Dorta,[b] Verónica Gonzalez-Nunez,[c] Katherine Barreto-Valer,[c] Filipa Marcelo,[d] Luis P. Calle,[d] Jesús T. Vázquez,[b] Raquel E. Rodríguez,[c] Jesús Jiménez-Barbero[d] and Gregorio Valencia*[a]

Received 4th February 2011, Accepted 31st May 2011
DOI: 10.1039/c1ob05197k

To examine if the biological activity of the N/OFQ peptide, which is the native ligand of the pain-related and viable drug target NOP receptor, could be modulated by glycosylation and if such effects could be conformationally related, we have synthesized three N/OFQ glycopeptide analogues, namely: [Thr^{5}-*O*-α-D-GalNAc-N/OFQ] (glycopeptide **1**), [Ser^{10}-*O*-α-D-GalNAc]-N/OFQ (glycopeptide **2**) and [Ser^{10}-*O*-β-D-GlcNAc]-N/OFQ] (glycopeptide **3**). They were tested for biological activity in competition binding assays using the zebrafish animal model in which glycopeptide **2** exhibited a slightly improved binding affinity, whereas glycopeptide **1** showed a remarkably reduced binding affinity compared to the parent compound and glycopeptide **3**. The structural analysis of these glycopeptides and the parent N/OFQ peptide by NMR and circular dichroism indicated that their aqueous solutions are mainly populated by random coil conformers. However, in membrane mimic environments a certain proportion of the molecules of all these peptides exist as α-helix structures. Interestingly, under these experimental conditions, glycopeptide **1** (glycosylated at Thr-5) exhibited a population of folded hairpin-like geometries. From these facts it is tempting to speculate that nociceptin analogues showing linear helical structures are more complementary and thus interact more efficiently with the native NOP receptor than folded structures, since glycopeptide **1** showed a significantly reduced binding affinity for the NOP receptor.

Introduction

The nociceptin/orphanin FQ peptide (N/OFQ) was the first peptide discovered by reverse pharmacology. N/OFQ is the endogenous ligand for the NOP receptor,[1,2] which belongs to the G-protein-coupled receptor superfamily. Both ligand and receptor

[a]*Instituto de Química Avanzada de Cataluña (IQAC-CSIC), Barcelona, Spain. E-mail: gregorio.valencia@iqac.csic.es; Fax: +34 93 2045904; Tel: +34 934006113*
[b]*Instituto Universitario de Bio-Orgánica "Antonio González", Departamento de Química Orgánica, Universidad de La Laguna, La Laguna, Tenerife, Spain*
[c]*Department of Biochemistry and Molecular Biology, Faculty of Medicine, Instituto de Neurociencias de Castilla y León (INCyL), University of Salamanca, Spain*
[d]*Chemical and Physical Biology, Centro de Investigaciones Biológicas (CIB-CSIC), Madrid, Spain*

† Electronic supplementary information (ESI) available: HRMS, NMR and CD data of the N/OFQ and N/OFQ glycopeptide analogues (**1–3**). See DOI: 10.1039/c1ob05197k

‡ Abbreviations: Boc, *tert*-butoxycarbonyl; CD, circular dichroism; CSI, chemical shift indexes; DCM, dichloromethane; DIC, *N*,*N*′-diisopropylcarbodiimide; DIEA, *N*,*N*-diisopropylethylamine; DMEM, Dulbecco's Modified Eagle Medium; DMF, *N*,*N*-dimethylformamide; dr: *Danio rerio*; drNOP, zebrafish NOP receptor; Fmoc, *N*-fluorenyl-9-yl-methoxycarbonyl; FmocGln(Trt) Wang resin, N^{α}-Fmoc-N^{δ}-trityl-L-glutamine 4-benzyloxybenzyl ester polymer-bound; Fmoc-Ser[*O*-α-D-GalNAc(OAc)$_3$]OH, *O*-(2-acetamido-2-deoxy-3,4,6-tri-*O*-acetyl-α-D-glucopyranosyl)-*N*-α-(fluoren-9-yl-methoxycarbonyl)-L-serine; Fmoc-Ser[*O*-beta-D-GlcNAc(OAc)$_3$]OH, *O*-(2-acetamido-2-deoxy-3,4,6-tri-*O*-acetyl-β-D-glucopyranosyl)-*N*-α-(fluoren-9-yl-methoxycarbonyl)-L-serine; Fmoc-Thr[*O*-α-D-GalNAc(OAc)$_3$]OH, *O*-(2-acetamido-2-deoxy-3,4,6-tri-*O*-acetyl-α-D-glucopyranosyl)-*N*-α-(fluoren-9-yl-methoxycarbonyl)-L-threonine; Gal, *O*-β-D-galactopyranose; GalNAc, 2-deoxy-2-acetamido-*O*-β-D-galactopyranosylamine; GlcNAc, 2-deoxy-2-acetamido-*O*-β-D-glucopyranosylamine; HOBt, 1-hydroxybenzotriazole; HRMS, high resolution mass spectrometry; i.c.v., intracerebroventricular; N/OFQ, nociceptin/orphanin FQ peptide; [^{3}H]N/OFQ, (leucyl-3,4,5-^{3}H)-nociceptin/orphanin FQ peptide; NMR, nuclear magnetic resonance; NOESY, nuclear Overhauser enhancement spectroscopy; NOP, nociceptin receptor; Pmc, 2,2,5,7,8-pentamethyl-chroman-6-sulfonyl; PyBOP, benzotriazole-1-yl-oxy-tris-pyrrolidino-phosphonium hexafluorophosphate; rmsd, root-mean-square deviation; RP-HPLC, reverse phase high-performance liquid chromatography; SAR, structure–activity relationship; Ser(*O*-α-D-GlcNAc), *O*-(2-acetamido-2-deoxy-α-D-glucopyranosyl)-L-serine; Ser(*O*-β-D-GlcNAc), *O*-(2-acetamido-2-deoxy-β-D-glucopyranosyl)-L-serine; SPPS, solid phase peptide synthesis; *t*-Bu, *tert*-butyl; TFA, trifluoroacetic acid; TFE, trifluoroethanol; Thr(*O*-α-D-Glc), *O*-(α-D-glucopyranosyl)-L-threonine; Thr(*O*-α-D-GlcNAc), *O*-(2-acetamido-2-deoxy-α-D-glucopyranosyl)-L-threonine; TIS, triisopropylsilane; TOCSY, total correlation spectra; Trt, Trityl. *Abbreviations* used for amino acids and designation of peptides follow the rules of the IUPAC-IUB Commission of Biochemical Nomenclature in *J. Biol. Chem.* **1972**, *247*, 977-983.

are widely distributed in the central nervous system and in the spinal cord,[3,4] but N/OFQ also elicits physiological responses in the cardiovascular and immune systems, gastrointestinal and urogenital tracts and airways.[5,6] Early studies on the central nervous system demonstrated that N/OFQ modulates nociception, although such effects are hard to interpret and appear to depend on a number of factors, including the route of administration.[5] Thus, the hyperalgesia initially reported in the hot plate and tail flick assays after i.c.v. administration,[1,2] has since been reclassified as an antianalgesic effect.[7,8] Besides, i.c.v. administration of this peptide can functionally antagonize the analgesic effects of morphine and other opioids,[5,7,8] whereas N/OFQ has been shown to produce analgesia and/or to potentiate morphine analgesia after intrathecal administration.[5–7,9] Other actions of N/OFQ in the central nervous system include anxiolytic-like effects, which have been reported in several behavioural paradigms in animal models.[6,10,11] In addition to this, N/OFQ modulates several neurotransmitter systems such as glutamate, catecholamines and tachykinins[12–14] and is involved in higher brain functions, including learning, memory, attention, emotion and sensory perception.

Since NOP as well as opioid receptors are G-protein-coupled receptors, when N/OFQ interacts with its receptor, it activates several intracellular effectors such as adenylyl cyclase inhibition, blockade of Ca^{2+} channels,[1,2] and activation of protein kinases and K^+ channels.[6] However, N/OFQ shows low affinity and negligible activity at opioid receptors, and opioid ligands have low affinity for the NOP receptor, except for dynorphin A.[15] In addition, NOP receptors do not bind the opioid antagonist naloxone. For these reasons, the NOP receptor is currently classified as a non-opioid member of the opioid receptor family.

Although the involvement of N/OFQ in such a wide range of biological functions including pain, cardiovascular control and immunity may seem an obstacle for the development of selective drugs, the NOP receptor is currently considered a viable drug target.[16] Thus, considerable effort has been invested by the pharmaceutical industry in developing selective NOP ligands; for example, the screening of a library of 52 millions of ligands has led to the identification of five hexapeptides, which are now widely accepted as NOP receptor standards.[17] Additionally, important contributions to N/OFQ pharmacology have been made by academic groups, most notably by G. Calo and R. Guerrini.[18–24]

A long-standing cooperative research project in our laboratories has been aimed at the study of pain mechanisms and SAR studies on opioid ligands. Given that glycosylation causes important changes in the native conformation, stability, activity and processing of many proteins,[25] we have been exploring the glycoconjugate approach for the rational drug design of new opioids. Thus, after examining the effects exerted by simple sugars on the activity of some opioids, we have discovered new glycoconjugates with potent antinociceptive properties.[26,27] These results are in line with similar glycoconjugation modifications in other biologically active peptides.[28] As this approach had not yet been applied to the full native N/OFQ peptide, the aim of this work was to see if the biological activity of the native N/OFQ ligand could be modulated by glycosylation and if such effects were conformationally related. To do so, three different glycosylated N/OFQ analogues and the parent peptide were prepared. They were tested for biological activity in competition binding assays using the zebrafish animal model since we have previously characterized the zebrafish opioid receptors and propeptides, including pronociceptin, and found that the opioid neurotransmitter system is fully functional and has been broadly conserved during the course of vertebrate evolution.[29] The structural analysis of these glycopeptides by NMR and circular dichroism indicate that glycosylation elicits conformational changes in N/OFQ that correlate with ligand affinity.

Results and discussion

Design of analogues

Two subsequence definitions have been reported in the full sequence of N/OFQ. A first *N*-terminal segment (FGGF), termed the "message", seems primarily responsible for triggering stimulation of the receptor. The rest of the sequence, called the "address", (TGARKSARKLANQ) appears to be involved in binding and receptor specificity.[18] Another important feature of N/OFQ is a pharmacophore site that was proposed using NMR and bioactivity relationship data.[30] The site is defined by the spatial disposition of residues Phe^1, Phe^4 and Arg^8.

Two obvious *O*-glycosylation sites in the N/OFQ sequence are the Thr^5 and Ser^{10} positions. Thr^5 is at the hinge between the "message" and the "address", joining the two parts together and sitting next to a vertix (Phe^4) of the proposed pharmacophore site. On the other hand, Ser^{10}, which is located at the "address", is flanked by the two identical highly cationic tripeptide clusters Ala-Arg-Lys. Owing to the highly strategic positions occupied by Thr^5 and Ser^{10} in the N/OFQ sequence, they were chosen as the glycosylation points.

The preferred choices for the saccharide part were α and β-, *N*-acetylgalactosamine and *N*-acetylglucosamine as these sugars are involved in many important biological phenomena.[25] The selected glycoside and peptide combinations are shown in Fig. 1.

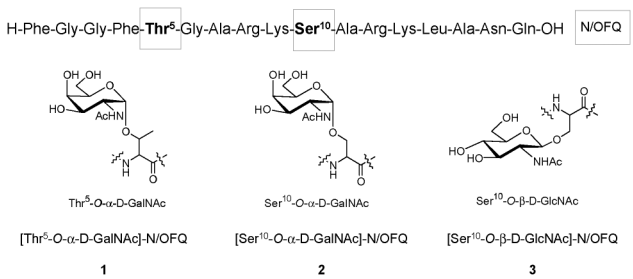

Fig. 1 Structure of the N/OFQ glycopeptides.

Glycopeptide **1** was designed to assess the influence of the presence of a sugar moiety at position 5 and glycopeptides **2** and **3** to test the combined effect of the nature of the sugar (GlcNAc *vs.* GalNAc) and the configuration of the glycosidic bond (α *vs.* β).

Synthesis of analogues

The preparation of glycopeptides **1–3** required the synthesis of three different glycosyl amino acid building blocks suitable for solid phase synthesis. The most demanding task was the preparation of those with a glycosidic bond in the α-configuration: Fmoc-Ser[*O*-α-D-GalNAc$(OAc)_3$]OH and Fmoc-Thr[*O*-α-D-GalNAc$(OAc)_3$]OH. This was successfully

accomplished following the nitroglycal method developed by Schmidt[31] and improved in our laboratories[32] by the use of methyl esters as efficient orthogonal carboxylic acid protecting groups and the introduction of a mild and selective methyl ester deprotection step effected by lithium iodide. In addition, this protecting group allowed the nitro group to be reduced with Zn in acid solution, instead of hydrogen and the unstable platinized RANEY® nickel. The Fmoc-Ser[*O*-β-D-GlcNAc(OAc)$_3$]OH building block was prepared by glycosylation of FmocSerOH with peracetylated GlcNAc using boron trifluoride etherate catalysis according to our own procedures.[33]

The three N/OFQ glycopeptides and the control N/OFQ peptide were manually assembled using these glycosyl amino acid building blocks by following standard Fmoc protocols of solid phase peptide synthesis, and were purified by RP-HPLC and characterized by HRMS.

Pharmacological properties of glycosylated nociceptin analogues

The biological characterization of the different nociceptin derivatives was achieved using radioligand binding techniques. The native nociceptin peptide and the three glycosylated analogues were tested as unlabelled ligands in competition binding experiments using drNOP membrane homogenates. The four peptides were able to effectively displace [^{3}H]-N/OFQ binding, and in all cases data fitted better to the one-site competition model (Fig. 2). According to their K_i values, the rank order of affinity was as follows: glycopeptide **2** (K_i value = 3.81 ± 0.19 nM) > nociceptin (N/OFQ) (K_i value = 7.99 ± 1.02 nM) > glycopeptide **3** (K_i value = 10.44 ± 2.56 nM) > glycopeptide **1** (K_i value = 54.95 ± 9.76 nM).

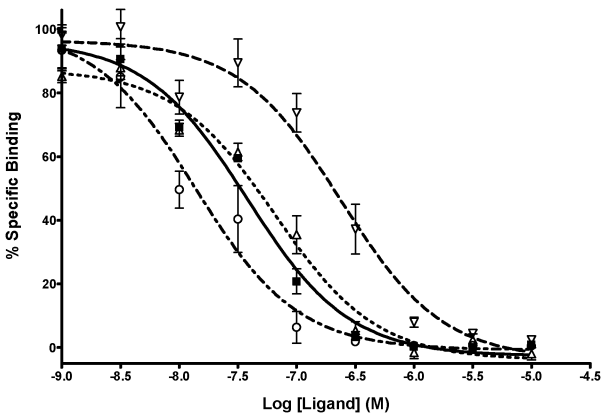

Fig. 2 Pharmacological properties of glycosylated nociceptin analogues. Competition binding experiments using [^{3}H]-N/OFQ and the glycosylated nociceptins (glycopeptides **1**, **2**, and **3**) together with the parent peptide on drNOP membrane homogenates. Data were fitted to the one-site competition model and each point represents the mean ± SEM (capped bars) of three independent experiments performed in triplicate. Legend: ■: N/OFQ (K_i = 7.99 ± 1.02 nM); ▽: glycopeptide **1** = [Thr^5-*O*-α-D-GalNAc]-N/OFQ (K_i = 54.95 ± 9.76 nM); ○: glycopeptide **2** = [Ser^{10}-*O*-α-D-GalNAc]-N/OFQ (K_i = 3.81 ± 0.19 nM); △: glycopeptide **3** = [Ser^{10}-*O*-β-D-GlcNAc]-N/OFQ (K_i = 10.44 ± 2.56 nM).

These results indicate that glycosylation of N/OFQ has different effects on the binding affinity of this endogenous ligand to the drNOP receptor. In fact, it seems that ligand affinity was affected not only by the glycosylation site, but also the nature of the glycosyl residue and glycosidic bond. Most notably, identical modifications (α-GalNAc) at Thr^5 and Ser^{10} (glycopeptide **1** *vs.* glycopeptide **2**) produced opposite effects on the K_i value of N/OFQ: glycopeptide **2** displayed a slightly lower K_i value than the parent peptide N/OFQ, while glycopeptide **1** showed a stronger affinity reduction for the drNOP receptor. In turn, β-GlcNAc glycosylation at Ser^{10} (glycopeptide **3**) did not significantly affect ligand affinity. These results are in accordance with the fact that modifications in the "address" might modulate peptide affinity. Moreover, the reduction of affinity observed for glycopeptide **1** may also be related to the steric disruption of the proposed N/OFQ pharmacophore (Phe^1/Phe^4/Arg^8) at the Phe^4 position and provide further proof of the important role of this residue in N/OFQ activity.[34]

Studies of N/OFQ glycosylation have been previously conducted only on the truncated and amidated N/OFQ (1–13)-NH$_2$ peptide.[35] This paper describes the synthesis of four *O*-β-glycosyl peptides and of two related acetylated intermediates. The two truncated Thr^5 glycosylated analogues show far lower biological activity (IC_{50} values on the mouse vas deferens preparations) than the other two glycoconjugates at Ser^{10}. These findings are in agreement with the biological activity reported here for our native N/OFQ glycopeptides.

Structural studies

Synthetic glycosylation of biologically active peptides has often been sought as a means of improving their pharmacology and ADME profiles. Given that these objectives are mostly achieved because sugar residues are able to modulate the bioactive conformations of peptides, we conducted a set of comparative structural studies on our N/OFQ glycopeptides to assess a possible structure–activity relationship (SAR).

In molecular recognition studies, it is usually assumed that the bioactive conformation of a given ligand is a well-defined geometry highly complementary to the receptor binding site. Such a definition implies that this conformation can only be observed when the proper ligand–receptor interactions take place. However, in the case of membrane receptors such as NOP and opioid receptors it is likely that ligand binding may be preceded by lipid membrane interaction events like those postulated by membrane compartment theories.[36] Accordingly, the lipid phase of a cellular membrane may act as a matrix for the receptor as well as the ligand.[37] Theoretical studies of receptor–ligand interactions in the context of membrane compartmentalization have provided support for this hypothesis,[38] suggesting that the initial interaction involves the adsorption of the ligand to the lipid membrane. In turn, such an insertion can induce a specific membrane-bound conformation that may be close to the bioactive conformation. For these reasons, we thought it would be of interest to study the solution conformation of our glycopeptides in membrane mimic environments using two different techniques. A low dielectric media, the organic solvent trifluoroethanol (TFE) that promotes secondary structure formation,[39] was used to examine the conformation of the glycopeptides by circular dichroism. As a more accurate membrane model for the study of peptide membrane interactions, SDS micelles were used for conformational studies of the glycopeptides by NMR techniques.[39–41] For comparative purposes, we also conducted NMR and circular dichroism studies in water.

Far-UV circular dichroism studies

The circular dichroism spectra of the glycopeptides and the parent N/OFQ in water or phosphate buffered saline solutions (pH 7.4) showed a negative Cotton effect just below 200 nm, which is indicative of random structure (Fig. 3A). When these spectra were recorded at increasing concentrations of TFE to simulate a more hydrophobic media,[39–41] three Cotton effects were observed, one positive at 195 and two negative at 205 and 222 nm (Fig. 3B). This pattern is indicative of a secondary structure order and characteristic of α-helix.[42]

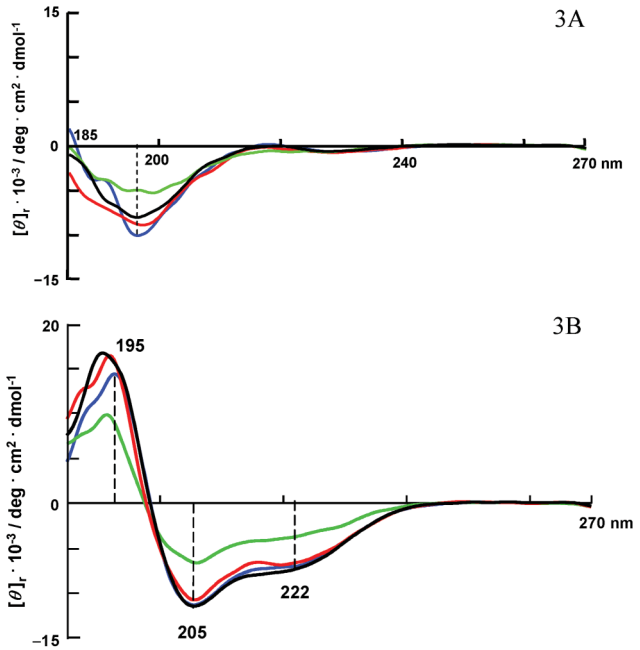

Fig. 3 3A) CD spectra of nociceptin (black) and glycopeptides **1** (red), **2** (blue), and **3** (green) in water. 3B) CD spectra of nociceptin (black) and glycopeptides **1** (red), **2** (blue), and **3** (green) in TFE.

In addition, the intensity ratio between the Cotton effects at 205 and 222 nm ($[\theta]_{222}/[\theta]_{205}$) has been associated with the tendency of a given peptide or protein to adopt helical structures.[43] Values of around 0.8 to 0.95 correspond to compounds with a tendency to yield high proportions of α-helix. For our glycopeptides and their parent compound in pure TFE solutions, these values were around 0.6, which meant their tendency to yield α-helix structures was low. This data can be further quantified taking into account that the absorption at 222 nm of a perfect α-helix is up to one order of magnitude more intense than a random or β-sheet presenting compound.[44] This is why the average ellipticity value observed at 222 nm can be taken as a measure of the proportion of α-helix in a sample. There are different model equations for the lineal relationship between the ellipticity of a sample at 222 nm and the estimated value of α-helix. We used the Luo and Baldwin model[45] to calculate α-helix proportions (*f*% values) of around 25% for N/OFQ and the glycopeptides **1** and **2**, and 15% for glycopeptide **3** (Table 1), the latter showing 40% less of the secondary ordered structure than the former. This reduction implies that the difference of nearly one order of magnitude in binding affinity between glycopeptides **1** and **2** cannot be solely explained in terms of the relative presence of α-helix conformers. Nevertheless, the same chemical modification (α-GalNAc) either at Thr[5] (glycopeptide **1**) or Ser[10] (glycopeptide **2**) of N/OFQ seems to retain the same α-helix conformer population as the parent N/OFQ peptide. Moreover, the CD data obtained for glycopeptide **3** is indicative of the importance of the stereochemistry of the sugar moiety in the conformational properties of these glycopeptides.

Table 1 CD Data of nociceptin and glycosylated nociceptin analogues and percentage of α-helix (*f*)

Peptide	$[\theta]_{195}$	$[\theta]_{205}$	$[\theta]_{222}$	*f* (%)
N/OFQ	16572	−11484	−7399	26
1	16333	−10817	−6681	24
2	14243	−11375	−7088	25
3	9762	−6727	−3827	15

NMR studies in aqueous solutions

Nociceptin has been structurally elusive and early biophysical studies have confirmed its tendency not to form well-defined structures in water and other polar solvents.[46] These studies have also revealed that the N/OFQ secondary structure in water, as examined by NMR, appears to be random, with rapid conformational interconversion at NMR time scales. Indeed, under our experimental conditions (see S.I. Tables S1–S4), the NMR data for N/OFQ and the glycopeptides (observed NOEs and $^3J_{HH}$ coupling constants from G6 to Q17) indicated that none of these compounds show well-defined secondary structures. As described in S.I. Figures S1–S4, very few long range NOEs could be detected. Also, in good agreement with recent reports,[30] the parent N/OFQ peptide, particularly its *N*-terminal part, seems to be rather flexible. Besides the sequential NOEs, very few inter residual NOEs could be observed. Those detected at the *C*-terminus seem indicative of the presence of a nascent α-helix in water solution. Nevertheless, the introduction of a sugar moiety at Thr[5] or Ser[10] produced a slight increase in the number of observed NOEs. Although merely qualitative, glycosylation at Ser[10] permitted a larger number of NOEs to be detected than at Thr[5], suggesting that this *O*-Ser substitution induced a certain rigidity of the peptide chain. On the other hand, no major changes in the chemical shifts of the different amino acid residues, other than those expected by glycosylation, were observed. This evidence allowed us to conclude that besides subtle modifications in the dynamic behaviour of the peptide chain upon glycosylation, there were no important structural changes, and that the glycopeptides mainly adopted disordered conformations in water. This result is in complete agreement with those obtained by CD analysis.

NMR studies in SDS micelles

As mentioned above, a further aim of this work was to explore if membrane compartment theories could apply in the case of N/OFQ and its glycopeptides. Thus, in order to deduce the possible bioactive conformation of these molecules, NMR experiments on glycopeptides **1–3** and N/OFQ were conducted, using SDS micelles as mimics of membrane-like environments[30,47] (see S.I. Tables S5–S8). Under these conditions, a significant increase in the number of NOE cross peaks, especially arising from NH–NH contacts, was observed for all tested compounds (see S.I. Figures S5). In the NOE assignment process, difficulties were

encountered due to the duplication of the Ala-Arg-Lys sequence at 7–9 and 11–12 positions. Nevertheless, the two distinct triads could be differentiated by assigning key NOEs for contacts between the 7–9 motif and the *N*-terminal region, as well as between the *C*-terminal part and the 11–12 repeated sequence. The rather small values for most $J_{NH\text{-}CH\alpha}$ coupling constants, together with the detection of typical α-helix NOE patterns, was initially interpreted as proof of the presence of a certain proportion of helical structures in N/OFQ and the glycopeptide micellar samples. These findings are in agreement with those reported by Mayo and co-workers and with our above-mentioned CD data in TFE for the natural analogue.[30] These α-helix-type NOE contacts were observed for all the peptide chains, including the FGGF message region at the *N*-terminus (see S.I. Figures S6–S9). This is the case, for instance, in the NOEs Hβ2 Asn^{16}-Hδ Lys^{13}, Hβ3 Asn^{16}-Hα Lys^{13}, Hα Leu^{14}-Hβ Gln^{17} and Hγ Gln^{17}, Hδ Leu14-Hγ Gln^{17}, Hγ Arg^{12}-Hα Lys^{9} and Hγ Lys^{9}-Hδ Arg,^{12} which correspond to the N/OFQ parent peptide (see S.I. Figure S10). However, some differences in the NOE patterns could be detected at Gly^{2} in all the different analogues and at the Ala^{7} position of glycopeptide **1** (see below).

Conformation–activity relationship

The initial perspective provided by the above reported NOE patterns suggests that helical structures are actually present for all these molecules. We also estimated the chemical shift indexes (CSI), which measure the deviation from random coil values of the different backbone α protons (Hα). As reference values to calculate the Hα CSIs, the literature values reported for the random coil chemical shifts of the different amino acids were used.[48] As reference values for the CSIs of the glycosylated positions, the reported values for non-glycosylated Ser and Thr residues in random coil were employed in a first approximation. In all cases, the data were in agreement with the presence of certain populations of α-helix structures, especially at the *C*-terminus, but with different lengths depending on the particular peptide.

However, in principle, this ubiquitous presence of α-helix does not explain the differences in affinity for the NOP receptor observed among the studied analogues. The Thr^{5} analogue (glycopeptide **1**) is the most notorious compound of this series, showing an affinity value of more than one order of magnitude smaller than that measured for the parent compound. In this context, the NOESY spectrum of glycopeptide **1** in SDS micelles revealed some key contacts not detected in the spectra of the other three peptides. Indeed, remote contacts between residues 4, 5, and 7 with the *C*-terminus 17 amino acid could be clearly identified. In particular, non ambiguous NOEs between Hε21 Gln17 and NH, Hα, Hβ and Hγ of Thr5, Hε21 Gln17-NH Ala 7 and Hε Gln17-Hβ2 Phe4 were detected, as shown in S.I. Figure S11. These data can only be explained by the presence of folded structures for glycopeptide **1**, which could not be detected for the other analogues (see below). The presence of a folded structure can be tentatively related with the presence of the α-GalNAc glycosylation at Thr^{5}. Indeed, folded structures seem to be an intrinsic structural feature of Thr residues when they are glycosylated by α-GalNAc.[49] Interestingly, glycopeptide **1** still preserves the characteristic NOE pattern of an α-helix structure at its *C*-terminus, suggesting that the observed folding is compatible with a certain population of a helix moiety between residues 14 and 17.

It should be emphasized that these remote contacts were only found for glycopeptide **1** but not for the parent peptide or for the other analogues, substituted at Ser^{10} by either β-GlcNAc or α-GalNAc. These molecules do not show any secondary structural features other than those related to the presence of a certain percentage of α-helix.

Glycopeptide modeling

It is well known that *O*-glycosylation of Ser and Thr has a profound effect on the conformation of the underlying peptide backbone,[50] however, such effect may be context dependent.[51,52] This effect also regulates the 3D-orientation of the sugar attached to Ser or Thr, and therefore, the study of the bioactive conformation of a given glycopeptide obviously requires the careful analysis of both the conformation of the peptide backbone and the orientation of the sugar. Thus, 3D models of the glycopeptides were built employing the experimental NMR data by using a standard protocol of combined automated NOE assignment and structure calculations employing the CYANA program[53] (see S.I., Table S9, for the statistics of the NMR solution structures of the N/OFQ peptide and glycopeptides **1–3**).

The 3D model for N/OFQ and glycopeptide 2

Fig. 4 shows the estimated Hα CSI values and the calculated 3-D model for the parent peptide (N/OFQ) and glycopeptide **2**. Inspection of the Hα CSI values for both peptides indicates that several residues from Ala7 to Gln17 seem to be integrated within a helical structure. Indeed, as discussed above, the analysis of

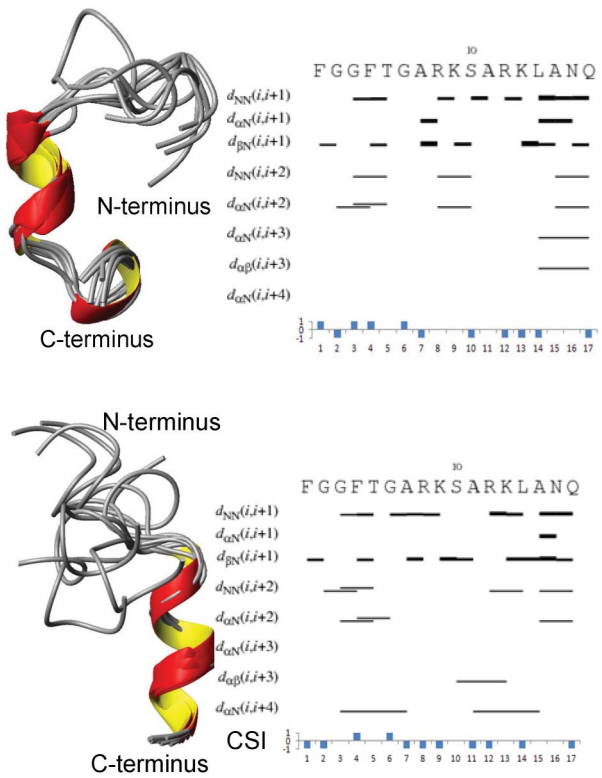

Fig. 4 Superimposition of 8 selected structures, NOE connectivities and Hα chemical shift index (CSI) for nociceptin (N/OFQ) and the Ser^{10}-*O*-α-D-GalNAc glycopeptide **2**.

the NOE connectivities indicated that Ser[10]-*O*-α-D-GalNAc has additional $i/i + 4$ NOE contacts. Accordingly, it seems that α-GalNAc glycosylation of Ser[10] does not affect the helical structure of the parent nociceptin. Furthermore, the analysis of the ϕ/ψ values of the 20 structures obtained by CYANA with respect to the peptide backbone of the Lys-Ser-Ala triad showed that the spatial disposition of these three residues is in good agreement with a major α-helix structure. (See S.I. in Figures S12 and S13 for the Ramachandran plots obtained by CYANA for these peptides).

In the case of glycopeptide **2**, further conformational analysis of the glycosidic torsion angles provided evidence that, in accordance with the *exo*-anomeric effect, ϕ_g (O5–C1–O1–Cβ) was restricted at around 60°, while ψ_g (C1–O1–Cβ–Cα), besides being more flexible, displayed a major anti-arrangement for the GalNAc residue.[48] In contrast, $\chi 1$ (N2–Cα–Cβ–O1) seems to be much more flexible. In fact, two different orientations around this torsion angle ($\chi 1 = 60°$ and $\chi 1 = -150°$) were observed in solution (Fig. 5), which were experimentally supported by the exclusive NOE cross-peaks assigned for each conformation in the NOESY spectra (see S.I., Figure S14 and S15).

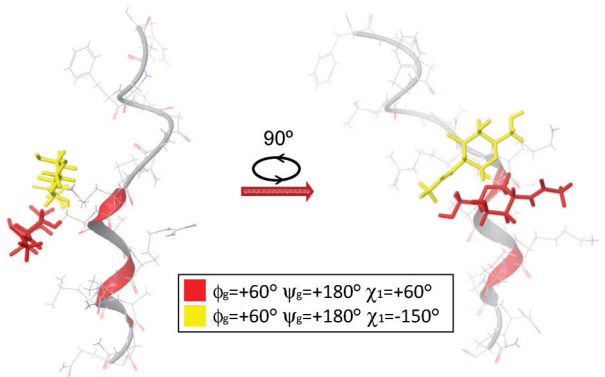

Fig. 5 Superimposition of the 3D view of the model structures for glycopeptide **2** (Ser[10]-*O*-α-D-GalNAc) with $\chi 1 = 60°$ and $\chi 1 = -150°$. The two distinct orientations of the GalNAc moiety are evident.

The 3D model for glycopeptide 3

As already discussed, the initial analysis of the NMR data for glycopeptide **3**, showing a Ser[10]-*O*-β-D-GlcNAc modification, revealed that more than one structural motif was again present in solution. Indeed, the 3D model shown in Figure S16 shows that, in spite of the presence of a helical structure at the *C*-terminus, the flexibility of the glycopeptide remains very high. Such an increase of flexibility after glycosylation is reflected by the values of ϕ and mainly ψ dihedral angles of the peptide backbone (see S.I. Figure S17). The analysis of these torsion angles with respect to the Lys-Ser-Ala triad also allowed us to verify that, in contrast to the observations for peptide N/OFQ and glycopeptide **2**, several conformers have a wide range of torsion angle values. This observation is in agreement with recent studies that have demonstrated that β-*O*-GlcNAc glycosylation on a Ser moiety introduces a higher flexibility around the glycosidic torsion angles ϕ_g, ψ_g and $\chi 1$ of the lateral chain if compared to Thr-β-*O*-GlcNAc.[54] In this case, two possible values of ϕ_g, correlated with minor fluctuations around ψ, were found. As expected, a remarkable flexibility around $\chi 1$ was observed for glycopeptide **3**. Thus, considering $\phi_g = 60°$ and $\psi_g = 180°$, only the combination of several $\chi 1$ values could explain the experimental NOE contacts. For instance, the conformation with $\chi 1 = -60°$ may explain the H8–NH Ser10 NOE, while $\chi 1 = 60°$ could account for the H4–NH Ser10 NOE. In turn, $\chi 1 = 180°$ is related to the H4–Hβ Ala 7 NOE. Therefore, *O*-Ser-β-D-GlcNAc glycosylation of nociceptin presents a high flexibility at the glycosylation site, somewhat extended along the peptide chain.

The 3D model for glycopeptide 1

The initial analysis of the NMR data discussed above supports that an α-*O*-GalNAc glycosylation at the Thr[5] residue of O/NFQ significantly affects the conformation of the peptide backbone. The unique experimental remote contacts observed for (Thr[5]-*O*-α-D-GalNAc) (see S.I. Figure S11) could only be explained by the presence of a folded conformation of glycopeptide **1** (Fig. 6 and in S.I. Figure S18). The structure calculations revealed a cluster of 8 folded hairpin-like conformers from the 20 best CYANA structures. The analysis of ϕ/ψ values (peptide backbone) of Thr[5] also located key changes in the secondary structure of this molecule. For glycopeptide **1**, the ϕ/ψ values are concentrated in the region of ppII in the Ramachandran plot, while for the parent O/NFQ peptide, the torsion angles are placed in the α-helix region. These confined values of ϕ_g, ψ_g and also of $\chi 1$ reduce the flexibility and consequently drive the peptide chain to adopt folded conformations (Fig. 6). This effect is also in agreement with the fact that rotation around the glycosidic linkage in

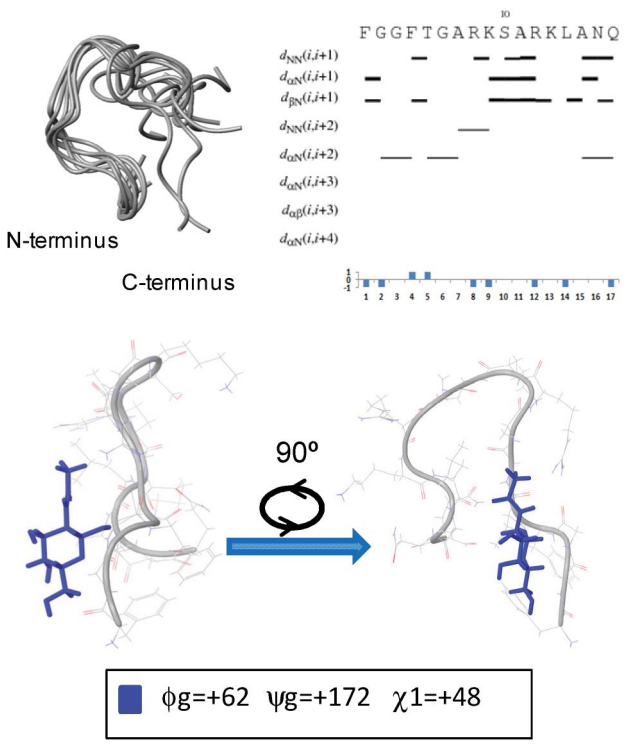

Fig. 6 Top left: Superimposition of 8 selected structures of the backbone of glycopeptide **1** (Thr[5]-*O*-α-D-GalNAc) according to the CYANA calculations, showing the folded structure. Top right panel: the NOE connectivities and the Hα chemical shift index (CSI) are shown. The orientation of the GalNAc residue *versus* the polypeptide chain is also shown at the bottom.

Thr-α-D-GalNAc moieties is restricted, a feature that does not take place in the Ser glycosylated analogues.[55]

Conclusions

The effect of *O*-glycosylation on the biological activity and secondary structure of native nociceptin has been examined for the first time by conjugation with GlcNAc and GalNAc monosaccharides. The pharmacological analysis of the three new glycopeptides revealed that N/OFQ glycosylation modulates the binding affinity of this endogenous ligand to the drNOP receptor. These effects were dependent on the glycosylation site as well as the nature of the linked monosaccharide.

Comparative structural analysis between the glycopeptides and the parent N/OFQ peptide by circular dichroism and NMR techniques indicated that in water solutions random conformations were mainly present. As seen by circular dichroism, upon addition of TFE, α-helix structures started to be populated for all peptides. In pure TFE solutions, the α-helix proportions were estimated to be around 25% except for glycopeptide **3**, which was only 15%. Under these experimental conditions, the differences in the proportion of α-helix do not correlate with the observed binding affinities of these compounds and do not account for the large decrease shown by glycopeptide **1**.

In good agreement with previous reports, our NMR studies have identified a certain degree of helical structure in the parent N/OFQ peptide micellar solutions of SDS. The observed NOE patterns for the glycopeptides suggest that α-helix motifs are also present in the membrane mimic media, although glycopeptide **3** seems to be more flexible than **2** and the parent compound. Fittingly, for glycopeptide **1**, a distinct set of remote contacts between the *N*- and *C*-termini were detected in the NOESY spectra, suggesting that this glycopeptide exhibits a significant population of folded hairpin-like structures. The experimental NMR data were employed to derive 3D models of these molecules, which showed the presence of differently extended α-helix sections for all of them, but also the presence of a unique folded conformation only for glycopeptide **1**. This distinct structural feature may be responsible for the observed reduced affinity of this molecule for the NOP receptor (nearly one order of magnitude). The difference in binding affinity for the other analogues could be related to their varying flexibility.

Finally, although on many occasions the relationships between structure and activity seem elusive, in this case it is tempting to justify that nociceptin analogues showing linear helical structures are more complementary and thus interact more efficiently with the native NOP receptor than folded structures. This hypothesis is initially supported by the evidence provided here for the different behaviour of N/OFQ and its Ser^{10} glycosylated analogues compared with those of Thr^{5}. In any event, structural studies of the binding of these molecules to NOP receptor preparations should shed further light on the interaction mechanisms and on the bioactive conformation of nociceptin. These studies are currently being performed in our laboratories.

Experimental

Materials

All amino acid building blocks, coupling reagents and prederivatized Fmoc Gln(Trt) Wang resin were purchased from Novabiochem AG. Other reagents including tri-*O*-benzyl-D-galactal and sodium dodecyl sulfate-d_{25} were purchased from Sigma-Aldrich (St Louis, MO). [^{3}H]-N/OFQ (82.3 Ci mmol^{-1}) was obtained from Perkin-Elmer (Boston, MA). All other reagents used were of analytical grade.

Peptide synthesis

Nociceptin peptide (N/OFQ) and the glycopeptides (**1**, **2**, and **3**) were synthesized manually by using standard N^{α}-Fmoc solid-phase methodology on a FmocGln(Trt) prederivatized Wang resin.[56] The required glycosyl amino acid building blocks were prepared using previously published methods.[31–33] N^{α}-Fmoc glycosyl amino acids (3 equiv.) were used. Side chain protecting groups used to build the glycopeptide sequences were the following: Trt for Gln and Asn, *t*Bu for Ser and Thr, Boc for Lys and Pmc for Arg. The FmocGln(Trt) Wang resin (1 equiv.) was placed in a glass peptide synthesis column with a frit on the bottom and swollen in DMF for 1 h. The amide couplings were effected by DIC (3 equiv.) and HOBt (6 equiv.). In the case of glycosylated building blocks (3 equiv.) couplings were effected using PyBOP (3 equiv.), HOBt (3 equiv.) and DIEA (6 equiv.). Each coupling was performed manually in this peptide synthesis column using DMF as a solvent under reciprocal oscillating agitation. The coupling efficiencies were monitored by the Kaiser ninhydrin test. The Fmoc groups were removed with a solution of 20% piperidine in DMF (1 × 9 min). The deprotected resin was washed with DMF, DCM, and then DMF. After assembling the glycopeptide sequence, a cocktail of TFA/TIS/H_2O (95 : 2.5 : 2.5) was used to remove the side chain protecting groups and to cleave the peptide from the resin. The crude glycopeptides were precipitated with ice-cold *tert*-butyl methyl ether, filtered, redissolved in water and lyophilized. The acetyl protecting groups on the sugar moieties were next hydrolyzed carefully adding sodium methoxide/MeOH solutions to methanol solutions of the protected glycopeptides (monitored by analytical reverse-phase HPLC). The glycopeptides were neutralized by addition of AcOH and concentrated under reduced pressure. The final glycopeptides were purified by RP-HPLC using acetonitrile–water gradient followed by lyophilization. The final pure peptides were characterized by HRMS.

Circular dichroism

CD spectra were obtained on a JASCO J-600 spectropolarimeter and recorded in the range of 270–185 nm by using a 1 mm cylindrical quartz cell. All spectra were recorded at room temperature, with a band width of 1.0 nm, and a step resolution of 0.2 nm. A sensitivity of 20 mdeg, a time constant of 2 s, a scan speed of 20 nm min^{-1}, and four scans were used. Prior to measurements, the spectropolarimeter was calibrated with a standard solution of ammonium *d*-camphor-10-sulfonate in distilled water. The molar ellipticities were determined using the formula $[\theta]_{n\rightarrow p^*} = \theta_{obs}MRW/[10lc]$, where the θ_{obs}. is in millidegrees, MRW is the mean residue molecular weight, l is the cell path length in cm, and c is the glycopeptide concentration in mg mL^{-1}. The α-helicity percentage (f) was determined by the Lifson–Roig helix–coil theory[57] and using the formula of Baldwin[45] % helix = $[\theta]_{n\rightarrow p^*}/[(-44\,000 + 250T)(1 - 3/n)]100$, where n represents the number of amide bonds (including *C*-terminal amide) in the

glycopeptide and $[\theta]_{n\rightarrow p^*}$ is molar ellipticity of n→p* transition band at 222 nm.

NMR Spectroscopy

Experiments were recorded in H_2O/D_2O 90 : 10 (phosphate buffer PBS pH = 6.7) on Bruker Avance 600 and 800 MHz spectrometers equipped with a triple channel cryoprobe and 278 K. NMR assignments were accomplished using standard 2D-TOCSY (mixing times of 20, 60, 80, and 100 ms), assisted by 2D-NOESY experiments (mixing times of 200 and 300 ms). The concentration of nociceptin and its glycopeptides for the NMR experiments varied from 1 to 2 mM. The pH for the nociceptin sample was adjusted to 5.4, and set at 6.7 for [Ser[10]-*O*-β-D-GlcNAc]-N/OFQ, [Ser[10]-*O*-α-D-GalNAc]-N/OFQ, [Thr[5]-*O*-α-D-GalNAc]-N/OFQ to properly monitor the amide hydrogens of the polypeptide backbone.

Additional NMR experiments were performed in the presence of SDS micelles to mimic a membrane-like environment. In this case, the experiments were recorded in H_2O/D_2O (90 : 10) on the same spectrometers and at 288 K. The NMR assignments were accomplished using the same experiments mentioned above. The concentration of nociceptin and its glycopeptides for the NMR experiments again varied from 1 to 2 mM, while the SDS concentration was 132 mM. The resonance of 2,2,3,3-tetradeutero-3-trimethylsilylpropionic acid (TSP) was used as a chemical shift reference in the ^{1}H NMR experiments (δTSP = 0 ppm).

Structure determination

Peak lists for the NOESY spectra (T = 288 K, 300 ms) recorded in presence of SDS micelles were generated by interactive peak picking using the CARA software.[58] NOESY cross-peak volumes were determined by the automated peak integration routine. The three-dimensional structure of nociceptin and its glycosylated derivatives was determined using the standard protocol of combined automated NOE (nuclear Overhauser effect) assignment and the structure calculation of the CYANA program (version 2.1).[53] Seven cycles of combined automated NOESY assignment and structure calculations were followed by a final structure calculation. The structure calculation started in each cycle from 100 randomized conformers, and the standard simulated annealing schedule was used.[59] The 20 conformers with the lowest final CYANA target function values were retained for analysis and passed to the next cycle. Weak restraints on glycosidic ϕ/ψ torsion-angle pairs and on side-chain torsion angles between tetrahedral carbon atoms were applied temporarily during the high-temperature and cooling phases of the simulated annealing schedule in order to favour the permitted regions of the Ramachandran plot and staggered rotamer positions respectively. The list of upper-distance bonds for the final structural calculation consists of unambiguously assigned upper-distance bonds and does not require the possible swapping of diastereotopic pairs. The resulting 20 CYANA conformers represent the ensemble average solution structure of nociceptin and analogues.

The MOLMOL program[60] was used to visualize the three-dimensional structures obtained by CYANA. CYANA was used to obtain statistics on target function values, restraint violations and Ramachandran plots. Root mean square deviation (rmsd) values were calculated using CYANA for superimpositions of the backbone N, Cα and C′ atoms, that is, the heavy atoms over the whole peptide. To obtain the rmsd of a structure represented by a bundle of conformers, all conformers were superimposed upon the averaged one and the average of the rmsd values between the individual conformers and their average coordinates was calculated.

Membrane preparation

Stably transfected HEK293 cells expressing the zebrafish NOP receptor (drNOP) were grown in DMEM (GibCo BRL, UK) medium supplemented with 10% fetal calf serum (GibC BRL, UK), 2 mM glutamine, 100 U mL^{-1} penicillin, 0.1 mg mL^{-1} streptomycin (BioWhitakker, Walkersville, MD) and 0.25 mg mL^{-1} Geneticin (GibCo BRL, UK) at 37 °C under a 5% CO_2 atmosphere. Cells were grown to 80% confluence, harvested in PBS pH 7.4 containing 2 mM EDTA and collected by centrifugation at 500*g*. The cell pellets were frozen at −80 °C for at least 1 h and resuspended in 50 mM Tris HCl buffer pH 7.4 (assay buffer) with protease inhibitors (0.1 mg mL^{-1} bacitracin, 3.3 μM captopril and protease inhibitor cocktail, from Sigma-Aldrich, St Louis, MO). The cell suspensions were homogenized with a Potter-Elvehjem tissue grinder with a Teflon pestle in assay buffer, the homogenates were centrifuged at 1500 rpm for 10 min at 4 °C. The nuclear pellet was homogenized again, centrifuged and discarded. The two supernatants were combined, homogenized again with the tissue grinder and the membrane pellet was collected upon centrifugation at 18000*g* for 30 min at 4 °C. The crude membrane fraction was resuspended in ice-cold assay buffer with protease inhibitors and protein concentration was determined by Bradford (BioRad).

Competition binding assays

The following unlabelled ligands were used: nociceptin (N/OFQ), the glycosylated nociceptin analogues: glycopeptide **1** [Thr[5]-*O*-α-D-GalNAc]-N/OFQ, glycopeptide **2** [Ser[10]-*O*-α-D-GalNAc]-N/OFQ, and glycopeptide **3** [Ser[10]-*O*-β-D-GlcNAc]-N/OFQ. 20–25 μg protein were incubated with different concentrations of unlabelled ligand ranging from 0.3 nM to 10 μM, and using [^{3}H]-N/OFQ as a radioligand (the working concentration was similar to the K_D). Reactions were incubated for 1 h at 25 °C in a final volume of 250 μL of assay buffer with (0.1 mg mL^{-1}) proteinase-free BSA to avoid the adsorption of the radioligand to the walls of the tubes. 10 μM nociceptin was used to determine nonspecific binding. After incubation, the reaction was stopped by adding 4 mL of ice-cold 50 mM Tris HCl buffer pH 7.4. The mixture was rapidly filtrated using a Brandel Cell Harvester and washed two times onto GF/B glass-fiber filters that were presoaked with 0.2% polyethylenimine for at least 1 h. The filters were placed in scintillation vials and incubated overnight at room temperature in EcoScint A scintillation liquid (London, England). Radioactivity was counted using a Beckman Coulter scintillation counter (Pasadena, CA). All experiments were performed in triplicate and repeated three times.

Data analysis

Specific binding was defined as the difference between total binding and nonspecific binding, as measured in presence of 10 μM unlabelled nociceptin. Data were analyzed using the Graph Pad Prism software (San Diego, CA) and inhibition constants (K_i-values) were calculated using the Cheng and Prusoff equation, which corrects for the concentration of radioligand used in each experiment as well as the affinity of the radioligand for its binding site (K_D).[61] In all cases, data were fitted to the one-site or two-site competition model, and compared by using the nonlinear least-squares curve-fitting which is based upon a statistical F-test.

Acknowledgements

The work was supported by a grant from the Fundació Marató de TV3 (Pain, project reference 070430-31-32-33). We thank F. J Cañada, M. Morando and L. Nieto for helpful discussions, and M. Bruix for the access to the 800 MHz NMR spectrometer. JJB acknowledges Ministerio de Ciencia e Innovación (Spain) (CTQ2009-08536) for financial support. F. M. thanks to FCT-Portugal for a post-doc research grant (SFRH/BPD/65462/2009). JTV acknowledges Ministerio de Ciencia e Innovación (Spain) (CTQ2007-67532-C02-02/BQU) for financial support. M. R. acknowledges a fellowship (AP2009-2534, Formación de Profesorado Universitario) from the Ministry of Education.

Notes and references

1 J. C. Meunier, C. Mollereau, L. Toll, C. Suaudeau, C. Moisand, P. Alvinerie, J. L. Butour, J. C. Guillemot, P. Ferrara and B. Monsarrat, *Nature*, 1995, **377**, 532–535.
2 R. K. Reinscheid, H. P. Nothacker, A. Bourson, A. Ardati, R. A. Henningsen, J. R. Bunzow, K. Grandy, H. Langen, F. J. Jr. Monsma and O. Civelli, *Science*, 1995, **270**, 792–794.
3 H. P. Nothacker, R. K. Reinscheid, A. Mansour, R. A. Henningsen, A. Ardati, F. J. Jr. Monsma, S. J. Watson and O. Civelli, *Proc. Natl. Acad. Sci. U. S. A.*, 1996, **93**, 8677–8682.
4 C. Mollereau and L. Mouledous, *Peptides*, 2000, **21**, 907–917.
5 J. S. Mogil and G. W. Pasternak, *Pharmacol. Rev.*, 2001, **53**, 381–415.
6 L. C. Chiou,Y. Y. Liao, P. C. Fan, P. H. Kuo, C. H. Wang, C. Reimer and E. P. Prinssen, *Curr. Drug Targets*, 2007, **8**, 117–135.
7 L. M. Harrison and D. K. Grandy, *Peptides*, 2000, **21**, 151–172.
8 J. E. Grisel and J. S. Mogil, *Peptides*, 2000, **21**, 1037–1045.
9 X. Xu, S. Grass, J. Hao, I. Shi Xu and Z. Wiesenfeld-Hallin, *Peptides*, 2000, **21**, 1031–1036.
10 F. Jenck, J. L. Moreau, J. R. Martin, G. J. Kilpatrick, R. K. Reinscheid, F. J. Jr. Monsma, H. P. Nothacker and O. Civelli, *Proc. Natl. Acad. Sci. U. S. A.*, 1997, **94**, 14854–14858.
11 E. C. Gavioli and G. Calo, *Naunyn-Schmiedebergs Arch. Pharmacol.*, 2006, **372**, 319–330.
12 B. Nicol, D. G. Lambert, D. J. Rowbotham, D. Smart and A. T. McKnight, *Br. J. Phamacol.*, 1996, **119**, 1081–1083.
13 M. Marti, S. Stocchi, F. Paganini, F. Mela, C. De Risi, G. Calo, R. Guerrini, T. A. Barnes, D. G. Lambert, L. Beani, C. Bianchi and M. Morari, *Br. J. Pharmacol.*, 2003, **138**, 91–98.
14 S. Giuliani and C. A. Maggi, *Br. J. Pharmacol.*, 1996, **118**, 1567–1569.
15 F. Meng, L. P. Taylor, M. T. Hoversten, Y. Ueda, A. Ardati, R. K. Reinscheid, F. J. Jr. Monsma, S. J. Watson, O. Civelli and H. Akil, *J. Biol. Chem.*, 1996, **271**, 32016–32020.
16 (*a*) D. G. Lambert, *Nat. Rev. Drug Discovery*, 2008, **7**, 694–710; (*b*) T. M. Largent-Milnes and T. W. Vanderah, *Expert Opin. Ther. Pat.*, 2010, **20**, 291–305.
17 C. T. Dooley, C. G. Spaeth, I. P. Berzetei-Gurske, K. Craymer, I. D. Adapa, S. R. Brandt, R. A. Houghten and L. Toll, *J. Pharmacol Exp. Ther.*, 1997, **283**, 735–741.
18 R. Guerrini, G. Calo, A. Rizzi, C. Bianchi, L. H. Lazarus, S. Salvadori, P. A. Temussi and D. Regoli, *J. Med. Chem.*, 1997, **40**, 1789–1793.
19 R. Guerrini, G. Calo, A. Rizzi, R. Bigoni, C. Bianchi, S. Salvadori and D. Regoli, *Br. J. Pharmacol.*, 1998, **123**, 163–165.
20 R. Guerrini, G. Calo, D. G. Lambert, G. Carrá, M. Arduin, T. A. Barnes, J. McDonald, D. Rizzi, C. Trapella, E. Marzola, D. J. Rowbotham, D. Regoli and S. Salvadori, *J. Med. Chem.*, 2005, **48**, 1421–1427.
21 M. Arduin, B. Spagnolo, G. Calo, R. Guerrini, G. Carrà, C. Fischetti, C. Trapella, E. Marzola, J. McDonald, D. G. Lambert, D. Regoli and S. Salvadori, *Bioorg. Med. Chem.*, 2007, **15**, 4434–4443.
22 G. Calo, R. Guerrini, R. Bigoni, A. Rizzi, G. Marzola, H. Okawa, C. Bianchi, D. G. Lambert, S. Salvadori and D. Regoli, *Br. J. Pharmacol.*, 2000, **129**, 1183–1193.
23 G. Calo, A. Rizzi, D. Rizzi, R. Bigoni, R. Guerrini, G. Marzola, M. Marti, J. McDonald, M. Morari, D. G. Lambert, S. Salvadori and D. Regoli, *Br. J. Pharmacol.*, 2002, **136**, 303–311.
24 G. Calo, R. Guerrini, A. Rizzi, S. Salvadori, M. Burmeister, D. R. Kapusta, D. G. Lambert and D. Regoli, *CNS Drug Rev.*, 2005, **11**, 97–112.
25 (*a*) L. L. Kiessling and R. A. Splain, *Annu. Rev. Biochem.*, 2010, **79**, 619–653; (*b*) A. Varki and J. B. Owe, Biological Roles of Glycans. In: *Essentials of Glycobiology*, ed. A. Varki, R. D. Cummings, J. D. Esko, H. H. Freeze, P. Stanley, C. R. Bertozzi, G. W. Hart and M. E. Etzler, Cold Spring Harbor Laboratory Press, Cold Spring Harbor (NY), 2nd edition, 2009, ch. 6.
26 R. E. Rodríguez, F. D. Rodríguez, M. P. Sacristán, J. L. Torres, G. Valencia and J. M. García Antón, *Neurosci. Lett.*, 1989, **101**, 89–94.
27 G. Arsequell, M. Salvatella, G. Valencia, G. A. Fernández-Mayoralas, M. Fontanella, Ch. Venturi, J. Jiménez-Barbero, E. Marrón and R. E. Rodríguez, *J. Med. Chem.*, 2009, **52**, 2656–2666.
28 (*a*) T. Yamamoto, P. Nair, N. Jacobsen, J. Vagner, V. Kulkarni, P. Davis, S. W. Ma, E. Navratilova, H. I. Yamamura, T. W. Vanderah, F. Porreca, J. Lai and V. J. Hruby, *J. Med. Chem.*, 2009, **52**, 5164–5175; (*b*) M. M Palian, V. I. Boguslavsky, D. F. O'Brien and R. Polt, *J. Am. Chem. Soc.*, 2003, **125**, 5823–5831; (*c*) T. Yamamoto, P. Nair, N. E. Jacobsen, P. Davis, S. W. Ma, E. Navratilova, J. Lai, H. I. Yamamura, T. W. Vanderah, F. Porreca and V. J. Hruby, *J. Med. Chem.*, 2008, **51**, 6334–6347; (*d*) E. J. Bilsky, R. D. Egleton, S. A. Mitchell, M. M. Palian, P. Davis, J. D. Huber, H. Jones, H. I. Yamamura, J. Janders, T. P. Davis, F. Porreca, D. J. Hruby and R. Polt, *J. Med. Chem.*, 2000, **43**, 2586–2590; (*e*) L. Negri, R. Lattanzi, F. Tabacco, B. Scolaro and R. Rocchi, *Br. J. Pharmacol.*, 1998, **124**, 1516–1522; (*f*) L. Negri, R. Lattanzi, F Tabacco, L. Orrù, C. Severini, B. Scolaro and R. Rocchi, *J. Med. Chem.*, 1999, **42**, 400–404.
29 V. Gonzalez-Nunez and R. E. Rodriguez, *ILAR J.*, 2009, **50**, 373–386.
30 M. K. Orsini, I. Nesmelova, H. C. Young, B. Hargittai, M. P. Beavers, J. Liu, P. J. Connolly, S. A. Middleton and K. H. Mayo, *J. Biol. Chem.*, 2005, **280**, 8134–8142.
31 (*a*) G. A. Winterfeld, Y. Ito, T. Ogawa and R. R. Schmidt, *Eur. J. Org. Chem.*, 1999, **5**, 1167–1171; (*b*) G. A. Winterfeld and R. R. Schmidt, *Angew. Chem., Int. Ed.*, 2001, **40**, 2654–2657; (*c*) A. L. Khodair and R. R. Schmidt, *Eur. J. Org. Chem.*, 2003, **6**, 1009–1021.
32 C. Mayato, R. L. Dorta and J. T. Vázquez, *Tetrahedron Lett.*, 2008, **49**, 1396–1398.
33 G. Arsequell, L. Krippner, S. Y. C. Wong and R. A. Dwek, *J. Chem. Soc., Chem. Commun.*, 1994, 2383–2384.
34 R. Guerrini, G. Caló, R. Bigoni, D. Rizzi, A. Rizzi, M. Zucchini, K. Varani, E. Hashiba, D. G. Lambert, G. Toth, P. A. Borea, S. Salvadori and D. Regoli, *J. Med. Chem.*, 2001, **44**, 3956–3964.
35 B. Biondi, D. Goldin, E. Giannini, R. Lattanzi, L. Negri, P. Melchiorri, L. Ciocca and R. Rocchi, *Int. J. Pept. Res. Ther.*, 2006, **12**, 139–144.
36 R. Schwyzer, *Biochemistry*, 1986, **25**, 6335–6342.
37 B. Gysin and R. Schwyzer, *Arch. Biochem. Biophys.*, 1983, **225**, 467–474.
38 G. Adam and M. Delbrück, Reduction of Dimensionality in Biological Diffusion Processes, in *Structural Chemistry and Molecular Biology*, ed. A. Rich and N. Davidson, W.H. Freeman and Co., San Francisco, 1968, pp. 198–215.
39 M. Buck, *Q. Rev. Biophys.*, 1998, **31**, 297–355.
40 X. Wei, S. Ding, Y. Jiang, X. G. Zeng and H. M. Zhou, *Biochemistry (Mosc.)*, 2006, **71** (Suppl. 1), S77–S82.

41 J. F. Povey, C. M. Smales, S. J. Hassard and M. J. Howard, *J. Struct. Biol.*, 2007, **157**, 329–338.
42 *Circular Dichroism and the Conformational Analysis of Biomolecules*, Ed. G. D. Fasman, Plenum Press, New York, 1996.
43 R. S. Kiss, C. M Kay and R. O. Ryan, *Biochemistry*, 1999, **38**, 4327–34.
44 (*a*) W. C. Johnson and I. Tinoco Jr., *J. Am. Chem. Soc.*, 1972, **94**, 4389–4392; (*b*) J. D. Morrisett, J. S. K. David, H. J. Pownall and A. M Gotto Jr, *Biochemistry*, 1973, **12**, 1290–1299; (*c*) P. C. Lyu, J. C. Sherman, A. Chen and N. R. Kallenbach, *Proc. Natl. Acad. Sci. U. S. A.*, 1991, **88**, 5317–5320; (*d*) J. M. Scholtz, H. Qian, E. J. York and J. M. Stewart, *Biopolymers*, 1991, **31**, 1463–1470; (*e*) K. L. Lazar, H. Miller-Auer, G. Getz, J. P. R. O. Orgel and S. C. Meredith, *Biochemistry*, 2005, **44**, 12681–12689.
45 P. Luo and R. L. Baldwin, *Biochemistry*, 1997, **36**, 8413–8421.
46 S. Salvadori, D. Picone, T. Tancredi, R. Guerrini, R. Spadaccini, L. H. Lazarus, D. Regoli and P. A. Temussi, *Biochem. Biophys. Res. Commun.*, 1997, **233**, 640–643.
47 (*a*) G. D. Henry and B. D. Sykes, *Methods Enzymol.*, 1994, **239**, 515–535; (*b*) P. Damberg, J. Jarvet and A. Gräslund, *Methods Enzymol.*, 2001, **339**, 271–285.
48 D. S. Wishart, C. G. Bigam, A. Holm, R. S. Hodges and B. D. Sykes, *J. Biomol. NMR*, 1995, **5**, 67–81.
49 F. Corzana, J-H. Busto, G. Jiménez-Osés, M. García de Luis, J. L. Asensio, J. Jiménez-Barbero, J. M. Peregrina and A. Avenoza, *J. Am. Chem. Soc.*, 2007, **129**, 9458–9467.
50 (*a*) M. R. Pratt and C. R. Bertozzi, *Chem. Soc. Rev.*, 2005, **34**, 58–68; (*b*) M. R. Wormald, A. J. Petrescu, Y. L. Pao, A. Glithero, T. Elliott and R. A. Dwek, *Chem. Rev.*, 2002, **102**, 371–386.
51 M. M. Palian, N. E. Jacobsen and R. Polt, *J. Pept. Res.*, 2001, **58**, 180–189.
52 L. K. Kreppel, M. A. Blomberg and G. W. Hart, *J. Biol. Chem.*, 1997, **272**, 9308–9315.
53 P. Güntert, *Methods Mol. Biol.*, 2004, **278**, 353–378.
54 A. Fernández-Tejada, F. Corzana, J. H. Busto, G. Jiménez-Osés, J. Jiménez-Barbero, A. Avenoza and J. M. Peregrina, *Chem.–Eur. J.*, 2009, **15**, 7297–7301.
55 H. Kogelberg, D. Solis and J. Jiménez-Barbero, *Curr. Opin. Struct. Biol.*, 2003, **13**, 646–653.
56 W. C. Chan and P. D. White, in *Fmoc Solid Phase Peptide Synthesis: A practical Approach*, ed. W. C. Chan and P. D. White, Oxford University Press, Oxford, 2000, pp. 41–76.
57 S. Lifson and A. Roig, *J. Chem. Phys.*, 1961, **34**, 1963–1974.
58 R. Keller, *Computer-aided Resonance Assignment Tutorial CARA*, Cantina Verlag, Goldau, Switzerland.
59 P. Günter, C. Mumenthaler and K. Wüthrich, *J. Mol. Biol.*, 1997, **273**, 283–298.
60 R. Koradi, M. Billeter and K. Wüthrich, *J. Mol. Graphics*, 1996, **14**, 51–55.
61 Y. Cheng and W. H. Prusoff, *Biochem. Pharmacol.*, 1973, **22**, 3099–3108.

